Original Research (2026) 3(2); 61- 70
https://doi.org/10.22103/VCBR.2026.26578.1116

Shahid Bahonar University of Kerman

Veterinary and Comparative Biomedical Research

ORIGINAL ARTICLE

Protective Effects of Tannic Acid–Loaded Selenium Nanoparticles against Peritoneal Adhesions via Regulating Oxidative Stress and Inflammatory Gene Expression

Moosa Javdani [1], Yalda Dourandish [1], Behnaz Karimi Babaahmadi [2*], Shima Balali Dehkordi [2]

[1] *Department of Clinical Sciences, Faculty of Veterinary Medicine, University of Shahrekord, Shahrekord, Iran*
[2] *Department of Basic Sciences, Faculty of Veterinary Medicine, University of Shahrekord, Shahrekord, Iran*

Online ISSN: 3060-7663 **https://doi.org/10.22103/VCBR.2026.26578.1116**

***Correspondence**

Author's Email:
Karimibabaahmadi@sku.ac.ir

Article History

Received: *22 December 2025*
Revised: *09 February 2026*
Accepted: *24 February 2026*
Published: *26 May 2026*

Keywords

Peritoneal Adhesion
Selenium Nanoparticles
Tannic Acid
Oxidative Stress
Inflammatory Gene

Abstract

Postoperative peritoneal adhesions remain a significant clinical challenge, often leading to serious complications such as chronic pain, intestinal obstruction, and infertility. Evidence indicates that oxidative stress and inflammation are key drivers of postoperative peritoneal adhesion formation. This study investigated the therapeutic potential of intraperitoneal administration of Tannic Acid (TA)-loaded selenium nanoparticles (SeNPs), in a rat model of surgically induced peritoneal adhesions. Thirty male Wistar rats (n=6 per group) were randomly divided into five groups to evaluate potential anti-adhesion therapies: sham (no adhesion induction), control (adhesion induction without treatment), SeNPs (1 mg/kg, single intraperitoneal (i.p.) dose after adhesion), tannic acid (TA, 20 mg/kg, single i.p. dose after adhesion), and a combination group (SeNPs + TA at the same doses, single i.p. dose after adhesion). All animals were killed 7 days later and cecum tissue samples were collected for biochemical and molecular analyses. Biochemical findings revealed a marked attenuation of oxidative stress, as evidenced by a significant decrease in xanthine oxidase activity and malondialdehyde levels in the SeNPs+TA group compared with the control group ($P < 0.05$). Gene expression analysis revealed a synergistic anti-inflammatory effect for the SeNPs+TA combination, which induced significantly greater downregulation of key pro-inflammatory mediators (particularly IL-1β and IL-6) compared to either monotherapy. At the level of upstream regulation, NF-κB expression followed a similar but non-significant decreasing trend, a finding that may reflect the limited duration of the single-dose treatment protocol. Collectively, these results suggest that tannic acid-loaded selenium nanoparticles exert potent antioxidant and anti-inflammatory actions, effectively targeting the principal molecular pathways involved in postoperative adhesion formation. Therefore, this combinatorial nanotherapeutic approach shows considerable promise as a therapeutic strategy for the management of postoperative peritoneal adhesions.

How to cite this article: Moosa Javdani, Yalda Dorandish, Behnaz Karimi Babaahmadi, Shima Balali Dehkordi. Protective Effects of Tannic Acid–Loaded Selenium Nanoparticles against Peritoneal Adhesions via Regulating Oxidative Stress and Inflammatory Gene Expression. *Veterinary and Comparative Biomedical Research*, 2026 3(2): 61 – 70. https://doi.org/10.22103/VCBR.2026.26578.1116

Introduction

Peritoneal adhesions are abnormal fibrous bands between tissues and organs, primarily resulting from peritoneal injury during surgery, infection, inflammation, or radiation (1). They form rapidly, often within 5–7 days, and occur in over 90% of patients after abdominal or pelvic operations (1, 2). Clinically, adhesions cause serious complications such as bowel obstruction, chronic pain, infertility, and organ injury. They also complicate future surgeries by increasing the risk of bowel perforation and extending operative time, presenting major clinical and economic challenges (3).

While the precise pathogenesis of postoperative peritoneal adhesions is not fully defined, their formation is generally attributed to an imbalance between fibrin deposition and degradation during peritoneal repair (4). The inflammatory response initiates this process, characterized by neutrophil and macrophage infiltration. These cells release cytokines, including IL-1β, TNF-α, TGF-β, and IL-6, into the injury site (3, 5). Proinflammatory cytokines, notably IL-1β and TNF-α, strongly induce NF-κB activation, which triggers adhesion progression by upregulating adhesion molecules such as E-selectin, ICAM-1, and VCAM-1 (6). These mediators, in turn, recruit more immune cells and stimulate mesothelial cell proliferation. Following the initial injury, tissue hypoxia, often accompanied by disrupted blood supply and subsequent reperfusion, triggers excessive reactive oxygen species (ROS) production, predisposing the peritoneum to adhesion development (7). Concurrently, fibrin deposits form a provisional matrix, leading to fibroblast infiltration and collagen deposition. By the second week, fibroblast activity decreases as mesothelial regeneration advances, resulting in mature fibrinous adhesions (5).

To address this issue, various pharmacological agents, such as fibrinolytics, anticoagulants, anti-inflammatory drugs, and antibiotics, have been widely studied and demonstrate promising therapeutic potential (8). However, their clinical efficacy is often limited by rapid systemic clearance. Furthermore, significant controversy surrounds the safety and effectiveness of certain therapies, particularly systemic fibrinolytics, due to the associated risks of postoperative hemorrhage and impaired tissue healing (9). Since adhesion formation is a multifactorial process primarily driven by inflammatory responses and oxidative stress, antioxidant and anti-inflammatory agents represent a critical strategy for its prevention and management (7). Indeed, nanotechnology has revolutionized therapeutic approaches by enhancing drug efficacy, reducing systemic toxicity, and enabling controlled release, thereby transforming treatment paradigms (10). Selenium nanoparticles (SeNPs), composed of elemental selenium (Se^0), offer a promising biomedical platform due to their favorable bioavailability and significantly reduced toxicity compared to other forms of selenium (10, 11).

SeNPs directly scavenge free radicals and enhance endogenous antioxidant defenses (11). They also potently suppress pro-inflammatory cytokines, demonstrating significant anti-inflammatory effects (12). Additionally, tannic acid (TA) is a water-soluble plant polyphenol with notable biological properties. Its structure features a D-glucose core fully esterified with galloyl groups, enabling potent free radical scavenging activity (13) .TA effectively inhibits migration and invasion in murine colon carcinoma cells by preserving tight junction integrity and downregulating key mesenchymal adhesion proteins, such as N-cadherin and integrins (14). In addition, TA has been effectively integrated into hydrogel systems for managing postoperative abdominal adhesions, where its anti-inflammatory activity underlies significant therapeutic efficacy (15). Building on this evidence, this study evaluates TA-loaded SeNPs as a novel strategy for preventing postoperative peritoneal adhesions in a rat model.

Materials and Methods

Synthesis of SeNPs and TA

Synthesis of the nanoparticles was performed according to the protocol previously reported by Shirian et al. (2024) (16). Briefly, 100 mg of chitosan was dissolved in 100 mL of a 1% (v/v) acetic acid solution, followed by the addition of 387 mg of ascorbic acid as a reducing agent. The mixture was stirred at 25 × g at room temperature, after which 5 mL of sodium selenite solution (11 mg/mL) was added dropwise under continuous stirring. The resulting SeNPs were collected by centrifugation, washed repeatedly with distilled water to remove unreacted precursors and residual reagents, and then re-dispersed prior to further physicochemical and analytical characterization.

Surface Modification of Nanoparticles Using TA

The synthesized SeNPs were resuspended in 30 mL of sterile normal saline. Surface functionalization was achieved by adding 600 mg of TA, followed by an esterification reaction conducted under continuous stirring for 24 h (overnight). Each experimental animal (rat) received a single dose of 0.25 mL of the final formulation, which contained 0.2 mg of SeNPs and 5 mg of TA per administered volume.

Animal Experimental Design

The study was approved by the Ethics Committee of Shahrekord University (Approval Code: IR.SKU.REC.1403.004). Thirty male Wistar rats, weighing 250–300 g and aged 6–8 weeks, were acclimatized for one week in stainless steel cages prior to experimentation. The animals were maintained under standard laboratory conditions, including a 12 h light/12 h dark cycle, a relative humidity of 65% ± 3%, and a controlled temperature of 23 ± 2 °C, with ad libitum access to standard rodent chow and water. Prior to intraperitoneal administration, all injectable solutions were sterilized by passage through a 0.22 µm sterile syringe filter under aseptic conditions. The rats were randomly allocated into five experimental groups (n = 6 per group) as follows: Group A (Sham) underwent a midline laparotomy without cecal abrasion. Group B (Control) was subjected to adhesion induction without any therapeutic intervention. Group C (SeNPs) received a single intraperitoneal injection of SeNPs (1 mg/kg, dissolved in 250 µL of sterile distilled water) immediately after adhesion induction, whereas Group D (TA) received a single intraperitoneal injection of TA (20 mg/kg, dissolved in 250 µL of sterile distilled water) immediately after adhesion induction. Group E (SeNPs–TA) received a single intraperitoneal injection of a combination of SeNPs (1 mg/kg) and TA (20 mg/kg), dissolved in 250 µL of sterile distilled water, following adhesion induction (17, 18). All animals were included in the experimental analyses, and no mortality or significant postoperative complications were observed throughout the experimental period.

Surgical Procedure

Anesthesia was induced by intraperitoneal administration of ketamine (70 mg/kg) and xylazine (10 mg/kg). After shaving and aseptic preparation of the abdominal area, rats were positioned supine, and the operative field was disinfected with a freshly prepared 1:20 povidone–iodine solution. A 3-cm midline laparotomy was performed to expose the cecum, which was gently exteriorized and kept moist with sterile saline-soaked gauze. A 2 × 1 cm serosal area of the cecum was abraded for 30 s using a sterile soft nylon dental brush to induce the cecal scratch model; the presence of petechial subserosal hemorrhages confirmed successful induction (16). The cecum was then returned to the abdominal cavity, and the assigned treatment was administered intraperitoneally as a single dose according to the experimental protocol. The abdominal wall was closed in two layers using absorbable 3-0 sutures. The animals were allowed to recover under standard conditions. One week postoperatively, the rats were euthanized by intraperitoneal administration of a ketamine–xylazine combination at a dose 10-fold higher than that used for anesthesia. The abdomen was then reopened via a U-shaped incision for blinded macroscopic evaluation, followed by the collection of cecal tissues for biochemical analyses and RNA extraction.

Biochemical Analysis in Cecal Homogenates

Cecal tissues were homogenized in ice-cold 0.1 M phosphate buffer (pH 7). Biochemical determinations were performed on the supernatants obtained after centrifugation of the homogenates at 18,000 × g for 3 min. These supernatants were subsequently used to assess xanthine oxidase (XO) activity and malondialdehyde (MDA) levels.

Evaluation of XO Activity

XO activity was measured using a commercially available assay kit (ZellBio GmbH, Ulm, Germany). This method is based on a coupled enzymatic reaction that produces a colorimetric signal measured at 575 nm, which is directly proportional to the amount of hydrogen peroxide generated during xanthine oxidation. One unit (U) of xanthine oxidase activity was defined as the amount of enzyme required to catalyze the oxidation of xanthine, resulting in the formation of 1 µmol of uric acid and hydrogen peroxide per minute at 25 °C, according to the manufacturer's instructions. XO activity was calculated using the following equation: Xanthine oxidase activity (U/mL) = $(OD_2 - OD_1) \times 800$ where OD_2 represents the absorbance of the sample and OD_1 represents the absorbance of the corresponding blank.

Protein Quantification in Cecal Tissue

Total protein concentration in the cecal tissue homogenates was determined using the Bradford colorimetric method (17). Briefly, 10 µL of the supernatant was mixed with 200 µL of Coomassie Brilliant Blue G-250 reagent, and absorbance was measured at 595 nm using a microplate reader. Protein concentrations were calculated from a standard calibration curve generated with bovine serum albumin (BSA) and expressed as milligrams of protein per milliliter. All biochemical parameters were subsequently normalized to the total protein content.

Determination of Malondialdehyde (MDA) Levels

MDA levels were determined according to the method of Peeri, et al. (2012) with minor modifications (20). Briefly, 1 mL of tissue homogenate was mixed with 2 mL of TBA reagent (15% trichloroacetic acid, 0.375% thiobarbituric acid, and 2.08 mL of 37.7% HCl), vortexed thoroughly,

transferred to sealed tubes, and heated in a water bath at 95 °C for 15 minutes. After cooling to room temperature, the samples were centrifuged at approximately 100 × g for 10 min, and the absorbance of the supernatant was measured at 535 nm. MDA concentration was calculated by dividing the absorbance measured at 535 nm by the molar extinction coefficient (1.56×10^5 M^{-1} cm^{-1}). The resulting value was then multiplied by 10^6 to convert the concentration to µM and normalized to tissue weight, and expressed as µM per mg of tissue.

Evaluation of NF-κB, IL-1β, IL-6, and TNF-α Gene Expression

Total RNA was extracted from 100 mg of cecal tissue using RNX-plus reagent (Yekta Tajhiz, Tehran, Iran) following the manufacturer's instructions. The purity and concentration of RNA were assessed by measuring optical density using a NanoDrop spectrophotometer, and the RNA was subsequently reverse-transcribed into cDNA using a commercial cDNA synthesis kit (Yekta Tajhiz Azma Co., Iran). The synthesized cDNA was stored at –70 °C until further use. Primers for each gene were designed using Allele ID software (Premier Biosoft, CA, USA) and validated by NCBI BLAST; their sequences, accession numbers, annealing temperatures, and product lengths are summarized in Table 1. For gene expression analysis, 2 µL of cDNA was mixed with 6 µL of 2X SYBR Green Master Mix and 0.5 µL of 5 mmol/L solutions of each forward and reverse primer in a final reaction volume of 12 µL. Quantitative real-time PCR was performed using a Roche qRT-PCR system (Roche Diagnostics, Mannheim, Germany) under the following conditions: initial denaturation at 95 °C for 10 min, followed by 40 cycles of 95 °C for 10 s, 60 °C for 20 s, and 72 °C for 20 s, with fluorescence detection at the end of each extension step. All reactions were performed in triplicate, and the specificity of PCR products was confirmed by melting curve analysis. Relative gene expression was calculated using the $2^{-\Delta\Delta Ct}$ method, with beta-actin serving as the housekeeping gene and internal control (21).

Statistical Analysis

All statistical analyses were performed using the SPSS software version 23.0 (SPSS Inc., Chicago, IL, USA). The data were expressed as mean ± SD. Statistical analysis was performed using One-way analysis of variance (ANOVA) followed by Tukey's post hoc tests for comparison of the means between the groups. A value of $P < 0.05$ was considered statistically significant.

Table 1. Primers for quantitative real-time PCR

Genes	Forward primer	Reverse primer
NF-kB	5′-AGCACCAAGACCGAAGCAA-3′	5′-TCTCCCGTAACCGCGTAGTC-3′
IL-1β	5′-GGAAGGCAGTGTCACTCATTGTG-3′	5′-GGTCCTCATCCTGGAAGCTCC-3′
IL-6	5'-GCCCTTCAGGAACAGCTATGA-3'	5'-TGTCAACAACATCAGTCCCAAGA-3'
TNF-α	5′AGCCCTGGTATGAGCCCATGTA3′	5′-CCGGACTCCGTGATGTCTAAGT-3′
Beta-actin	5'-GTCAGGTCATCACTATCGGCAAT-3'	5'-AGAGGTCTTTACGGATGTCAACGT-3'

Results

MDA Levels

As shown in Figure 1, MDA levels were significantly elevated in the control group relative to the sham group. In contrast, the combined treatment group showed a significant reduction in MDA compared to the control group ($P < 0.05$). Treatment with SeNPs or TA did alone not result in any significant differences compared to the control.

Assessment of XO Activity

Figure 2 demonstrates that XO activity was significantly elevated in the control group relative to the sham group. Treatment with either SeNPs–TA or selenium alone effectively attenuated this increase, resulting in a significant reduction in XO activity. Considering the central role of XO in catalyzing the production of reactive oxygen species, this pharmacological suppression of enzymatic activity likely represents a key mechanism for alleviating oxidative stress, a major contributor to the pathophysiology of the disease (22).

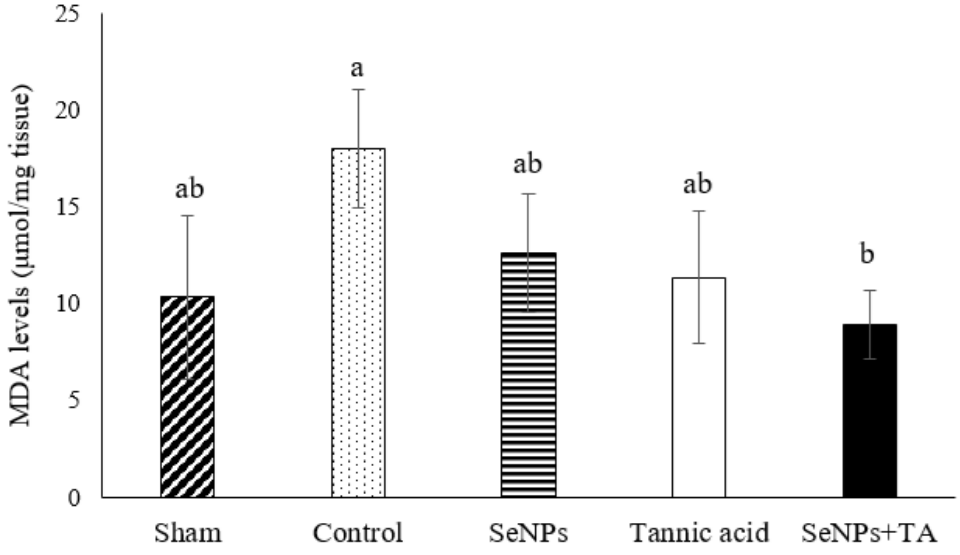

Figure 1: MDA levels in cacal tissue homogenate of rats at 7 days after the surgery-induced peritoneal adhesions in rats. Data are presented as mean ± SD. Different letters indicate significant differences among experimental groups, while * indicates a statistically significant difference compared with the control group ($P < 0.05$).

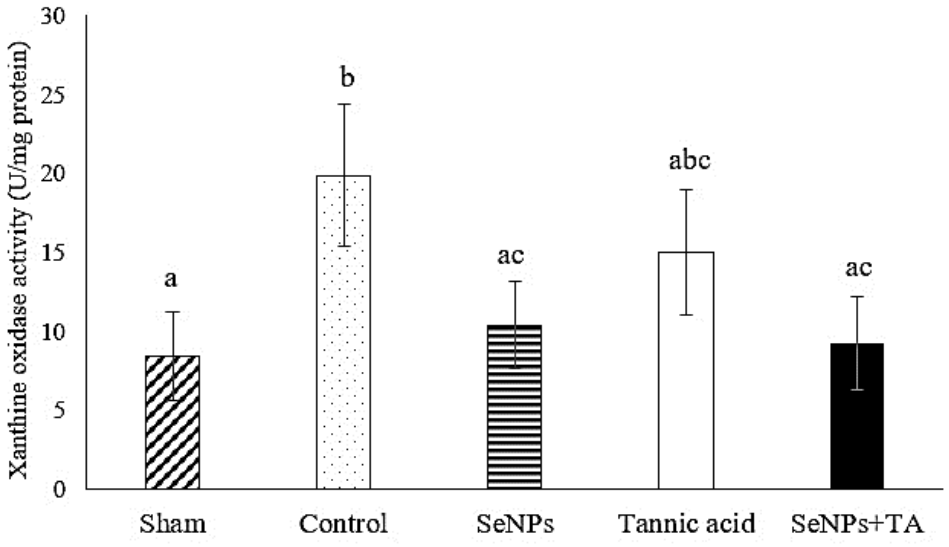

Figure 2: XO activity in cacal tissue homogenate of rats at 7 days after the surgery-induced peritoneal adhesions in rats. Data are presented as mean ± SD. Different letters indicate significant differences among experimental groups, while * indicates a statistically significant difference compared with the control group ($P < 0.05$).

Gene Expression Analysis

As illustrated in Figure 3, the control group exhibited a significant upregulation of the pro-inflammatory genes IL-1β, TNF-α, and IL-6 compared with the sham group ($P < 0.001$). Treatment with the SeNPs–TA intervention markedly attenuated the expression of all three genes relative to the control group ($P < 0.001$). Treatment with selenium and TA alone resulted in a significant reduction in TNF-α and IL6 gene expression compared with the control group ($P = 0.001$ and $P < 0.05$ respectively). However, the combined treatment of SeNPs–TA produced a more pronounced suppressive effect on IL-1β and IL-6 expression than either TA or SeNPs alone ($P \leq 0.05$). Evaluation of the relative expression of the NF-κB gene revealed no statistically significant differences between the treatment groups and the control group ($P > 0.05$).

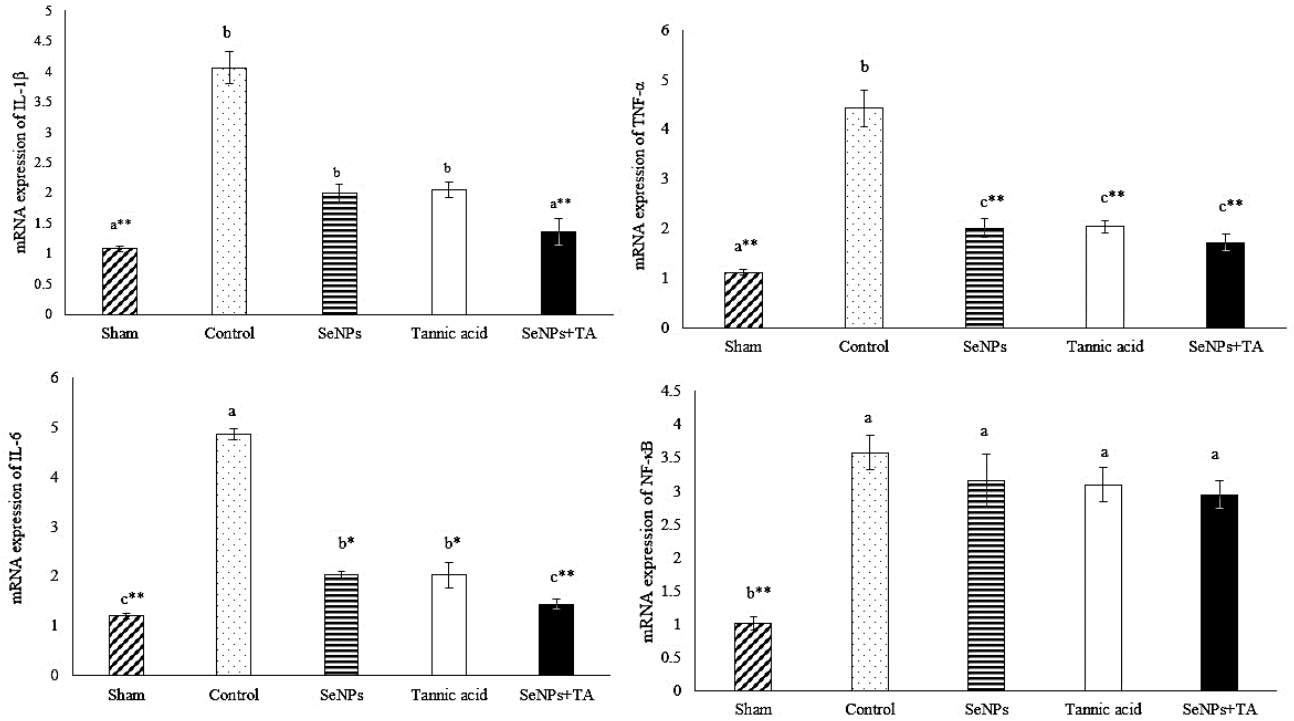

Figure 3: The mRNA expression levels of IL-1β, TNF-α, IL-6, and NF-κB in cecal tissue of different groups at 7 days after the surgery-induced peritoneal adhesions in rats. Data are presented as mean ± SD. Different letters indicate significant differences among experimental groups with *(*P* value < 0.05) and **(*P* value < 0.001) indicating statistically significant differences, respectively.

Discussion

In this study, the relative expression of NF-κB mRNA in cecal tissue was significantly higher in the control group compared with the sham group ($p < 0.001$), indicating activation of NF-κB in the early pathogenesis of peritonitis. NF-κB is a key nuclear transcription factor involved in the initiation and regulation of immune and inflammatory responses, promoting the transcription of pro-inflammatory cytokines such as TNF-α, IL-1β, and IL-6, particularly in macrophages (23). Consistent with our findings, Zhang et al. (2014) reported elevated NF-κB expression in inflammatory cells within peritoneal tissue during acute peritonitis (24).

In the present study, treatment with SeNPs, TA, and their combination resulted in a non-significant reduction in NF-κB gene expression compared with the control group. The persistence of a baseline level of NF-κB expression, even after treatment, is likely essential for its homeostatic roles in tissue repair, cellular proliferation, and angiogenesis, which are critical processes during the resolution of inflammation and adhesion formation (25). Thus, the observed non-significant reduction could reflect a balance between suppressing detrimental inflammation and preserving essential repair functions. This outcome is consistent with the established principle that the immunomodulatory effects of SeNPs are highly dependent on dose and treatment duration. For example, a pivotal study demonstrated that the short-term administration of SeNPs (14 days) increases the mRNA levels of TNF-α, IL-1β, IL-6, NF-κB, and SOCS3, whereas prolonged treatment (28 days) significantly reduces their expression (26). Given this evidence, the non-significant reduction in NF-κB expression observed here may be directly attributable to the short-term nature of our treatment protocol, which was limited to a single dose on the day of surgery.

Nevertheless, the NF-κB pathway remains a well-established and potent target for selenium-based interventions. Specifically, selenium is known to inhibit the binding of NF-κB to nuclear response elements, thereby downregulating the synthesis of pro-inflammatory cytokine mRNA (27). Furthermore, the close interconnection between NF-κB and other key signaling cascades, such as MAPK and JAK/STAT (28), means that targeting NF-κB with SeNPs can exert a broader anti-inflammatory effect by influencing these related pathways (28, 29). Notably, SeNPs have been shown to simultaneously inhibit MAPK, NF-κB, and STAT3 signaling, effectively disrupting the crosstalk among these critical pathways (29). In addition, interference with toll-like receptors (TLRs), which function as upstream activators of NF-κB signaling, has been proposed as another anti-inflammatory mechanism of nanoselenium (30).

Similarly, TA exerts potent anti-inflammatory effects by targeting the same key pathways. Its polyphenolic structure enables it to inhibit NF-κB and MAPK activation and suppress the production of inflammatory mediators (31). For example, it has been shown to attenuate dermatitis in murine models and reduce LPS-induced neuroinflammation in BV2 microglial cells through the inhibition of NF-κB signaling and pro-inflammatory cytokine production (32). Given these notable anti-inflammatory properties, it was hypothesized that a combination of SeNPs and TA would synergistically inhibit the production of major pro-inflammatory cytokines. Therefore, the expression of TNF-α, IL-6, and IL-1β was assessed in the experimental model. TNF-α plays a central role in initiating inflammatory and immune responses; however, its excessive production leads to sustained immune cell recruitment, chronic inflammation, and tissue damage (33). In this study, the expression levels of TNF-α, IL-6, and IL-1β were markedly increased in the control group following adhesion induction. In contrast, treatment with the combined SeNPs and TA group significantly reduced the expression of these pro-inflammatory genes compared with the control group. These findings indicate that the anti-inflammatory effects of SeNPs were potentiated by the concomitant anti-inflammatory activity of TA, highlighting the therapeutic potential of this combination in attenuating cecal tissue inflammation during peritonitis. Supporting these results, numerous studies have demonstrated that SeNPs inhibit the production of pro-inflammatory cytokines in various in vitro and in vivo inflammatory models (34, 35). Furthermore, SeNPs modulate immune cell function, particularly in macrophages, by promoting M2 macrophage polarization and suppressing the secretion of pro-inflammatory cytokines such as IL-1β and IL-10 (36). SeNPs have also been shown to ameliorate metabolic inflammation induced by a fructose-rich diet by reducing IL-1β, TNF-α, and IFN-γ levels and alleviating oxidative stress (37).

ROS play a crucial role in activating inflammatory signaling pathways and inducing tissue injury (38). The anti-inflammatory effects of nanoselenium may therefore be mediated, at least in part, through modulation of ROS production. Selenium, as a component of selenoproteins such as glutathione peroxidase (GPX) and thioredoxin reductase (TrxR), contributes to the attenuation of oxidative stress and the suppression of inflammation (34). By scavenging excessive ROS, selenium may prevent the direct activation of NF-κB or indirect activation via IκBα phosphorylation and DNA damage sensors such as ATM and ATR kinases (39). Xanthine oxidase (XO), the rate-limiting enzyme in purine catabolism, is a major source of ROS and plays an important role in immune responses and oxidative stress. Increased XO activity promotes NF-κB activation and subsequent release of pro-inflammatory cytokines (22). In the present study, XO activity was elevated in the control group following adhesion induction, whereas treatment with SeNPs, either alone or in combination with TA, significantly reduced XO activity. Selenium has also been shown to regulate oxidative stress in neutrophils by modulating TRPV1-mediated calcium influx, thereby reducing ROS generation and the activation of pro-oxidant enzymes such as XO (40). Consistent with these findings, Ghaffari et al. (2012) reported that combined vitamin E and sodium selenite supplementation modulates AO and XO activities (41). Although tannins exhibit weak to moderate direct XO inhibition, their antioxidant effects are primarily mediated through scavenging free radicals generated during enzymatic reactions (42).

Conclusion

The results of this study demonstrated that TA-loaded SeNPs exert remarkable effects in improving key parameters involved in adhesion formation. The superior efficacy of the combination treatment likely stems from a dual mechanism: the attenuation of oxidative stress markers and the downregulation of the pro-inflammatory cytokines. Despite these promising findings, the combined treatment did not produce a significant change in NF-κB expression, which may be attributable to the relatively short duration of the intervention. This limitation warrants further long-term investigation.

Acknowledgements

Not applicable.

Authors' Contributions

Moosa Javdani: Conceptualization, investigation, methodology, supervision, validation, visualization, writing and editing. **Yalda Dourandish:** Sample analysis**,** investigation and methodology, **Behnaz Karimi Babaahmadi:** Conceptualization, investigation, methodology, supervision, validation, visualization, writing – original draft, writing – review & editing. **Shima Balali Dehkordi:** formal analysis, investigation, methodology and writing.

Data Availability

All data analyzed during this study are included in this published article.

Ethical Approval

All applicable international, national, and/or institutional guidelines for the care and use of animals were followed.

Conflict of Interest

The authors affirm that there are no competing interests with the publication of this work.

Consent for Publication

Not applicable.

Funding

This study was not supported by any funding.

References

1. Whang SH, Astudillo JA, Sporn E, Bachman SL, Miedema BW, Davis W, et al. In search of the best peritoneal adhesion model: comparison of different techniques in a rat model. *J Surg Res*. 2011;15;167(2):245-50
2. Zhang H, Song Y, Li Z, Zhang T, Zeng L, Li W, et al. Evaluation of ligustrazine on the prevention of experimentally induced abdominal adhesions in rats. *Int Surg J*. 2015;1;21:115-21. https://doi.org/10.1016/j.ijsu.2015.06.081
3. Kakanezhadi A, Rezaei M, Raisi A, Dezfoulian O, Davoodi F, Ahmadvand H. Rosmarinic acid prevents post-operative abdominal adhesions in a rat model. *Sci Rep*. 2022; 3;12(1):18593. https://doi.org/10.1038/s41598-022-22000-x
4. Arung W, Meurisse M, Detry O. Pathophysiology and prevention of postoperative peritoneal adhesions. *WJG*. 2011;17(41):4545 https://doi.org/10.3748/wjg.v17.i41.4545
5. Zhang ZL, Xu SW, Zhou XL. Preventive effects of chitosan on peritoneal adhesion in rats. *World Journal of Gastroenterology: WJG*. 2006; 28;12(28):4572. https://doi.org/10.3748/wjg.v12.i28.4572
6. Lousse JC, Van Langendonckt A, González-Ramos R, Defrère S, Renkin E, Donnez J. Increased activation of nuclear factor-kappa B (NF-κB) in isolated peritoneal macrophages of patients with endometriosis. *Fertil Steril*. 2008;90(1):217-220. https://doi.org/10.1016/j.fertnstert.2007.06.015
7. Awonuga AO, Belotte J, Abuanzeh S, Fletcher NM, Diamond MP, Saed GM. Advances in the pathogenesis of adhesion development: the role of oxidative stress. *Reprod Sci*. 2014;21(7):823-36. https://doi.org/10.1177/1933719114522550
8. Khakzad MR. Effect of malva sylvestris extract on postoperative peritoneal adhesion in rats. *Jundishapur J Nat Pharm*. 2019;2(3):211-216. https://doi.org/10.7508/nmj. 2015.03.006
9. Mais V. Peritoneal adhesions after laparoscopic gastrointestinal surgery. *World Journal of Gastroenterology*. 2014;7;20(17):4917. https://doi.org/10.3748/wjg.v20.i17.4917
10. Karthik KK, Cheriyan BV, Rajeshkumar S, Gopalakrishnan M. A review on selenium nanoparticles and their biomedical applications. *Biomed Technol*. 2024:1;6:61-74. https://doi.org/10.1016/j.bmt.2023.12.001
11. Hosnedlova B, Kepinska M, Skalickova S, Fernandez C, Ruttkay-Nedecky B, Peng Q, et al. Nano-selenium and its nanomedicine applications: a critical review. *Int J Nanomedicine*. 2018:10:2107-28. https://doi.org/10.2147/IJN.S157541
12. Xing H, Bai X, Pei X, Zhang Y, Zhang X, Chen S, et al. Synergistic anti-oxidative/anti-inflammatory treatment for acute lung injury with selenium based chlorogenic acid nanoparticles through modulating Mapk8ip1/MAPK and Itga2b/PI3k-AKT axis. *J Nanobiotechnology*. 2025;23;23(1):37. https://doi.org/10.1186/s12951-025-03114-6
13. Sesia R, Ferraris S, Sangermano M, Spriano S. UV-cured chitosan-based hydrogels strengthened by tannic acid for the removal of copper ions from water. *Polym*. 2022; 1;14(21):4645. https://doi.org/10.3390/polym14214645
14. Barboura M, Cornebise C, Hermetet F, Guerrache A, Selmi M, Salek A, et al. Tannic acid, a hydrolysable tannin, prevents transforming growth factor-β-induced epithelial–mesenchymal transition to counteract colorectal tumor growth. *Cells*. 2022; 17;11(22):3645. https://doi.org/10.3390/cells11223645
15. Li Y, Liu G, Wang M, Zhang Y, You S, Zhang J, et al. The controlled release and prevention of abdominal adhesion of tannic acid and mitomycin C-loaded thermosensitive gel. *Polym*. 2023;16;15(4):975. https://doi.org/10.3390/polym15040975
16. Shirian S, Emamjomehzadeh P, Javdani M, Khosravian P, Karimi B. Investigating the Therapeutic Effects of Selenium Nanoparticles and Tannic Acid on Postoperative Peritoneal Adhesion in Rats. *J surg trauma*. 2025;10;13(4):144-53. http://dx.doi.org/10.61882/jsurgtrauma.13.4.144

17. Aiwale BS, Maurya R, Naqvi S. Green synthesized selenium nanoparticles mitigate cyclophosphamide-induced reproductive toxicity in male Wistar rats. *Naunyn Schmiedebergs Arch Pharmacol*. 2025;26:1-7. https://doi.org/10.21203/rs.3.rs-6759007/v1
18. Zhou XW, Liao ZF, Liu LM. Effects of tannic acid pretreatment on cardiovascular function during hemorrhagic shock in rats. Zhongguo wei Zhong Bing ji jiu yi xue Chinese Critical Care Medicine Zhongguo Weizhongbing Jijiuyixue. 2009;1;21(7):425-8
19. Mm B. A rapid and sensitive method for the quantitation of microgram quantities of protein utilizing the principle of protein-dye binding. Anal *Biochem*. 1976;72:248-54. https://doi.org/10.1016/0003-2697(76)90527-3
20. Peeri M, Haghigh MM, Azarbayjani MA, Atashak S, Behrouzi G. Effect of aqueous extract of saffron and aerobic training on hepatic non enzymatic antioxidant levels in streptozotocin-diabetic rats. *Archives Des Sciences*. 2012;65(10):525-32.
21. Livak KJ, Schmittgen TD. Analysis of relative gene expression data using real-time quantitative PCR and the 2(-Delta Delta C (T)) Method. *Methods*. 2001;25:402–8. doi: 10.1006/meth.2001.1262. https://doi.org/10.1006/meth.2001.1262
22. Chung HY, Baek BS, Song SH, Kim MS, Huh JI, Shim KH, Kim KW, Lee KH. Xanthine dehydrogenase/xanthine oxidase and oxidative stress. *Age*. 1997;20(3):127-40
23. Zhang T, Ma C, Zhang Z, Zhang H, Hu H. NF- κB signaling in inflammation and cancer. *MedComm*. 2021;2(4):618-53. https://doi.org/10.1007/s11357-997-0012-2
24. Zhang J, Wu Q, Song S, Wan Y, Zhang R, Tai M, et al. Effect of hydrogen-rich water on acute peritonitis of rat models. *Int Immunopharmacol*. 2014;21(1):94-101. https://doi.org/10.1016/j.intimp.2014.04.011
25. Bahrami A, Khalaji A, Bahri Najafi M, Sadati S, Raisi A, Abolhassani A, et al. NF-κB pathway and angiogenesis: insights into colorectal cancer development and therapeutic targets. *Eur J Med Res*. 2024;19;29(1):610. https://doi.org/10.1186/s40001-024-02168-w
26. Mal'tseva VN, Gudkov SV, Turovsky EA. Modulation of the functional state of mouse neutrophils by selenium nanoparticles in vivo. *Int J Mol Sci*. 2022;7;23(21):13651. https://doi.org/10.3390/ijms232113651
27. Chen KM, Spratt TE, Stanley BA, De Cotiis DA, Bewley MC, Flanagan JM, et al. Inhibition of nuclear factor-κB DNA binding by organoselenocyanates through covalent modification of the p50 subunit. *Cancer Res*. 2007;67(21):10475-83. https://doi.org/10.1158/0008-5472.CAN-07-2510
28. Chen L, Deng H, Cui H, Fang J, Zuo Z, Deng J, et al. Inflammatory responses and inflammation-associated diseases in organs. *Oncotarget*. 2017;9(6):7204. https://doi.org/10.18632/oncotarget.23208
29. Zaghloul RA, Abdelghany AM, Samra YA. Rutin and selenium nanoparticles protected against STZ-induced diabetic nephropathy in rats through downregulating Jak-2/Stat3 pathway and upregulating Nrf-2/HO-1 pathway. *Eur J Pharmacol*. 2022;15;933:175289. https://doi.org/10.1016/j.ejphar.2022.175289
30. Ye L, Liu S, Zhang X, Wang C, Li P, Zhang C, et al. Dietary nano-selenium improves health of liver and intestine of grass carp Ctenopharyngodon idella after overwintering. *A Anim Feed Sci. Technol.* 2023;1;306:115817. https://doi.org/10.1016/j.anifeedsci.2023.115817
31. Jing W, Xiaolan C, Yu C, Feng Q, Haifeng Y. Pharmacological effects and mechanisms of tannic acid. *Biomed Pharmacother*. 2022;154:113561. https://doi.org/10.1016/j.biopha.2022.113561
32. Wu Y, Zhong L, Yu Z, Qi J. Anti- neuroinflammatory effects of tannic acid against lipopolysaccharide-induced BV2 microglial cells via inhibition of NF- κB activation. *Drug Dev Res*. 2019;80(2):262-8. https://doi.org/10.1002/ddr.21490
33. Jang DI, Lee AH, Shin HY, Song HR, Park JH, Kang TB, et al. The role of tumor necrosis factor alpha (TNF-α) in autoimmune disease and current TNF-α inhibitors in therapeutics. *Int J Mol Sci*. 2021;8;22(5):2719. https://doi.org/10.3390/ijms22052719
34. Alkhudhayri AA, Dkhil MA, Al-Quraishy S. Nanoselenium prevents eimeriosis-induced inflammation and regulates mucin gene expression in mice jejunum. *Int J Nanomedicine*. 2018;3:1993-2003. https://doi.org/10.2147/IJN.S162355
35. Mi XJ, Le HM, Lee S, Park HR, Kim YJ. Silymarin-functionalized selenium nanoparticles prevent LPS-induced inflammatory response in RAW264. 7 cells through downregulation of the PI3K/Akt/NF-κB pathway. *ACS omega*. 2022;16;7(47):42723-32. https://doi.org/10.1021/acsomega.2c04140
36. Zhang F, Li X, Wei Y. Selenium and selenoproteins in health. *Biomolecules*. 2023; 8;13(5):799. https://doi.org/10.3390/biom13050799
37. Martínez-Esquivias F, Perez-Larios A, Guzmán-Flores JM. Effect of Administration of Selenium Nanoparticles Synthesized Using Onion Extract on

Biochemical and Inflammatory Parameters in Mice Fed with High-Fructose Diet: In Vivo and In Silico Analysis. *Biol Trace Elem Res*. 2024;202(2):558-68. https://doi.org/10.1007/s12011-023-03685-1

38. Mittal M, Siddiqui MR, Tran K, Reddy SP, Malik AB. Reactive oxygen species in inflammation and tissue injury. *Antioxid Redox Signal*. 2014;1;20(7):1126-67. https://doi.org/10.1089/ars.2012.5149
39. Hong Y, Boiti A, Vallone D, Foulkes NS. Reactive oxygen species signaling and oxidative stress: transcriptional regulation and evolution. *Antioxidants*. 2024;1;13(3):312. https://doi.org/10.3390/antiox13030312
40. Köse SA, Nazıroğlu M. Selenium reduces oxidative stress and calcium entry through TRPV1 channels in the neutrophils of patients with polycystic ovary syndrome. *Biol Trace Elem Res*. 2014;158(2):136-42. https://doi.org/10.1007/s12011-014-9929-3
41. Ghaffari T, Nouri M, Saei AA, Rashidi MR. Aldehyde and xanthine oxidase activities in tissues of streptozotocin-induced diabetic rats: effects of vitamin E and selenium supplementation. *Biol Trace Elem Res.* 2012;147(1):217-25. https://doi.org/10.1007/s12011-011-9291-7
42. Hatano T, YAsUHARA T, YosHIHARA R, AGATA I, NORO T, OkUDA T. Effects of interaction of tannins with co-existing substances. VII.: inhibitory effects of tannins and related polyphenols on xanthine oxidase. *Chem Pharm Bull*. 1990;25;38(5):1224-9. https://doi.org/10.1248/cpb.38.1224